Atomistic pseudopotential calculations of thickness-fluctuation GaAs quantum dots

Jun-Wei Luo,[1] Gabriel Bester,[2] and Alex Zunger[1]
[1]*National Renewable Energy Laboratory, Golden, Colorado 80401, USA*
[2]*Max-Planck-Institut für Festkörperforschung, D-70569 Stuttgart, Germany*
(Received 18 September 2008; revised manuscript received 1 December 2008; published 31 March 2009)

We calculate the electronic and optical properties of thickness-fluctuation quantum dots of different sizes and elongations using an atomistic empirical pseudopotential approach and configuration interaction. The carriers are confined by a monolayer fluctuation in the thickness of a $GaAs/Al_{0.3}Ga_{0.7}$

gations along the $[1\bar{1}0]$ direction have been reported.

IV. RESULTS FOR QUANTUM WELLS

Before we address the results for the thickness-fluctuation

V. CONFINEMENT POTENTIAL

In Fig. 3 we schematically illustrate the band edges of the materials involved in the TFQD. The reference energy is set to zero for the GaAs bulk VBM. The alloy barrier has conduction and valence-band edges at 1.924 and −0.150 eV, respectively. For the quantum well with 10 ML thickness, the conduction- and valence-band edges are at 1.662 and −0.044 eV, respectively. These numbers change to 1.650 and −0.040 eV for the 11 ML well. The hatched region in the Fig. 3 highlights the potential drop responsible for the confinement of electrons and holes in a TFQD with 10 ML nominal thickness. The electrons and holes are confined by only 12 and 4 meV, respectively. Only states within this energetic window can be confined in all three directions. Conduction (valence) -band states with energy between 1.662 and 1.924 eV (−0.044 and −0.150 eV) are quantum-well states confined in [001] direction but dispersive in-plane. Compared to the case of self-assembled InGaAs dots in GaAs with electron and hole confinement potentials of up to hundreds of meV, the situation is drastically different. Based on this qualitative analysis we expect states that tend to leak from the 11 ML dot region to the well region with 10 ML.

h_4 for the hole states. The smallest (20,20) TFQD has only one confined electron and one confined hole state while for the largest (100,20) TFQD four electron and four holes states are confined. The "shell structure," known from self-assembled quantum dots where the levels are grouped in *S*, *P*, *D* shells with degeneracy of 1,2,3, respectively, can be perceived for the (40,40) TFQD. However, for the smaller dots where only one level is confined and for the elongated dots there is no obvious pattern in the level spacings. The magnitude of the level spacings is an order of magnitude smaller than in self-assembled or colloidal quantum dots. The spacing between the first and second electron (hole) states in the (40,40) TFQD is only 5 (1) meV.

This can be seen as surprising, since the dimension of the TFQD is not very different than for some self-assembled quantum dots [e.g., 40 nm diameter and 3 nm height InGaAs/

Ba e e - a e (40,20) TFQD

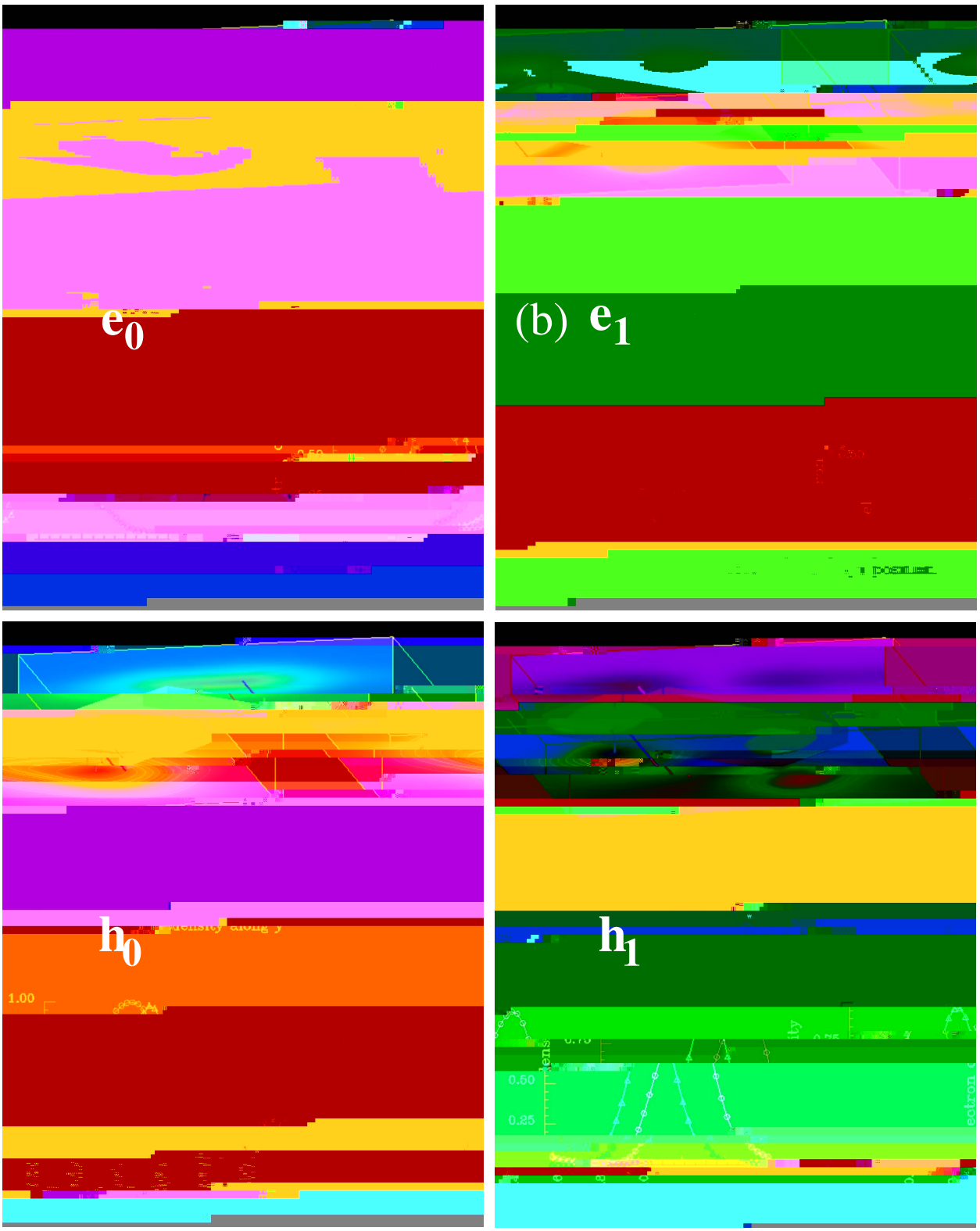

[redacted]

value significantly lower than for the (20,20) TFQD of similar dimensions. This is an additional indication that in spite of the similar sizes of the dots, the wave function occupies a significantly larger in-plane area in the case of the TFQD. The h_1 and h_2 states of Lens 1 dot are mixed hh-lh states due to the similar energetic position of h_1, h_2, and the light-hole band. The results for "Lens 2" quantum dot with large height (half sphere) is similar to Lens 1 case, with a hh dominant h_0 and mixed hh-lh h_1 and h_2 states, but for another reason. The large height leads to a smaller hh-lh splitting and despite the lower energetic position (around 20 meV above GaAs VBM) the hole states are energetically close to the lh band.

The calculations with the lens-shape dots illustrates the that hh-lh mixing is a consequence of (i) the lateral extent of the wave functions, controlling the energetic position of the states relative the quantum-well light-hole band, and (ii) the thickness of the well (dot, in Lens 1 and 2 cases) controlling the energetic position of the quantum-well light-hole band. For our TFQDs the large lateral extent of the wave functions and the narrow width of the well leads to almost pure heavy-hole states.

The benefit of the atomistic approach compared to a continuum description lies in a quantitative prediction of the effects described so far: (1) Continuum models rely on an external input for the potential, historically taken as a cylindrical potential[22,45] with certain band offsets and the results obtained are direct consequences of these assumptions. Our approach directly takes the shape of the structure as input parameter. (2) The penetration of states into the barrier is important since it governs the nature and the number of confined states, and requires the proper treatment of the interfaces and the matching of different types of Bloch functions, not given in a continuum description. (3) Another typical atomistic effect is the fact that alloy fluctuations in the barrier modify the distribution of wave functions significantlythe narrow w

TABLE II. Summary of the theoretical results for selected properties of $(GaAs)_{10}/Al_{0.3}Ga_{0.7}As$ TFQDs with different lateral dimensions (L_x, L_y) (nm^2) and experimental results.

Property	(20,20)	(40,20)	(40,40)	(100,20)	Expt.
X^0 (eV)	1.6902	1.6878	1.6851	1.6869	1.6813[a], 1.6886[b], 1.655[c]
X^{-1} (eV)	1.6893	1.6867	1.6841	1.6861	1.6856[b], 1.652[b]
$\Delta(X^0-X^{-1})$ (meV)	0.9	1.1	1.0	0.8	3.0[b]
δ_0 (μeV)	8	6	4	5	~100 [b,d]
δ_b (μeV)	0	5	0	4	~24 [a,d]
δ_d (μeV)	1	7	1	0	~1 [d]

[a]Reference 7.
[b]Reference 13.
[c]Reference 45.
[d]Reference 12.

including the transitions from the exciton (X), the biexciton (XX), and the charged trions (X^+, X^-). In Figs. 8(d)–8(f) we show the origin of the main transitions in the spectra [(a)–(c)] by giving the dominant configuration(s) of each level in parenthesis. We use the notation e_i^j and h_i^j where i is the index for the state and j the occupation of this state. Due to the few number of confined levels in the (20,20) TFQD (only one electron and one hole state) only few dot-to-dot transitions are possible leading to a very simple picture we omitted here. In the absorption spectra for the (40,20) and $(40,40)$ nm^2 TFQD [Fig. 8(a) and 8(b)] we can see a group of peaks around 1.685 and 1.687 eV. These transitions involve mainly the states e_0 and h_0 as can be seen in the analysis in Figs. 8(d) and 8(e). The transitions above 1.688 eV involve the higher excited states e_1, e_2, h_1, and h_2 and are well isolated from the first group of peaks. The situation is different in the case of the $(100,20)$ nm^2 TFQD [Fig. 8(c)] where all the transitions are grouped together between 1.687 and 1.692 eV. This smaller "bandwidth" of CI states is surprising considering that we are taking the same energy window for electrons and hole states as in the (40,20) and (40,40) cases. We will discuss this effect in Sec. XI. Another general observation is that the XX, X^+, and X^- transitions denoted by b_1, d_1, and c_1, respectively, are all redshifted with respect to the main X transition (a_1) in all calculated dots. In Fig. 9 we summarized calculations for the binding energy of the trions and biexcitons for three types of quantum dots. For TFQDs with one ML thickness fluctuation, TFQDs with two ML thickness fluctuations and for rectangular GaAs parallelepiped with height 11 ML fully embedded in $Al_{0.3}Ga_{0.7}As$. The results are plotted as a function of the exciton energy. The TFQDs with two ML thickness fluctuations have binding energies around 2 meV while it is around 1 meV for the TFQDs with 1 ML thickness fluctuations. The fully embedded quantum dots (Rect. QD) emit at higher energy and have between 2 and 2.5 meV binding energies.

For the case where no charged states are created and the excitation power is low enough to avoid the creation of biexciton, only the red lines in Figs. 8(a)–8(c) should be observed. We see two, three and four dominant peaks for the (40,20), (40,40), and (100,20), respectively. This represents a significant simplification from the single-particle picture with 16 possible transitions for the (40,40) and (100,20) TFQDs between confined states ($e_{0,1,2,3}$ and $h_{0,1,2,3}$ are confined). We will see that correlations are responsible for this simplification in Sec. XI. We note also that for the (40,40)

TABLE III. Summary of experimental results on TFQDs.

TFQDs	X^0 (eV)	$\Delta(X^0-X^{-1})$ (meV)	$\Delta(X^0-XX)$ (meV)	FS (μeV)	Note
$(GaAs)_{10}/Al_{0.3}Ga_{0.7}As$	1.6813[a], 1.6886[b] 1.655[c]	3.0[b] 3.0[c]	3.4[c]	$\delta_b(E_0)=-25$ [a], $\delta_b(E_1)=41$ [a], $\delta_b(E_2)=45$ [a], $\delta_b(E_3)=-22$ [a] $\delta_b(E_4)=-47$ [a] $\delta_0\sim 100$ [b,d], $\delta_d\sim 1$ [d], $\delta_b\sim 24$ [d]	$\Delta(E_1-E_0)=2.5$ meV [a] $\Delta(E_2-E_1)=1.0$ meV [a] $\Delta(E_3-E_2)=0.5$ meV [a] $\Delta(E_4-E_3)=0.5$ meV [a]
$(GaAs)_{12}/Al_{0.35}Ga_{0.65}As$	1.6586[e]	3.2[e]			
$(GaAs)_{10}/Al_{0.33}Ga_{0.67}As$	1.6977[f], 1.687[g], 1.6988[h]		2.7[f] 2.6[h]		$t_X=100$ ps [f], $t_{XX}=60$ ps [f], $f=75$ [f]
$(GaAs)_{15}/Al_{0.3}Ga_{0.7}As$	1.6280[b] 1.6212[i]	3.4[c]	3.36[i]		
$(GaAs)_{22}/Al_{0.3}Ga_{0.7}As$	1.5936[b], 1.663[k] 1.585[j]	3.5[k]			NSOM[j]
$(GaAs)_{30}/Al_{0.3}Ga_{0.7}As$	1.5598[b]				
$(GaAs)_{50}/Al_{0.3}Ga_{0.7}As$	1.5356[b]	1.2[b]			
$(GaAs)_{10}/Al_{0.33}Ga_{0.67}As$	1.6796		4.0[l]		

[a]Reference 7.
[b]Reference 13.
[c]Reference 45.
[d]Reference 12.
[e]Reference 2.
[f]Reference 5.
[g]Reference 15.
[h]Reference 6.
[i]Reference 14.
[j]Reference 11.
[k]Reference 17.
[l]Reference 10.

dot, where the attempt to label the states as *S*, *P*, and *D*, might seem justified, the transition a_2 is clearly visible, despite its dominant *S*-*P* character. Transitions of that type are mostly forbidden in self-assembled quantum dots.[42] For the negative trion, we calculate three dominant transitions for the (40,20) and (40,40) dots and seven for the (100,20) dot. For the positive trion we only see two dominant peaks for all the dot sizes. This qualitative difference emphasizes again the different nature of the electron and hole states despite the dominant single-band character of both electrons and holes.

XI. EFFECT OF CORRELATIONS

To illustrate the effect of correlations onto the optical properties of TFQDs we use the example of the excitonic transitions in the (100,20) TFQD. In Fig. 10 we present three different levels of approximation. At the first level only the single-particle energies, as given in Fig. 4, are considered. In Fig. 10(a) the resulting single-particle gaps are given as bar chart. In the next level the direct and exchange Coulomb interactions are included within each configuration 4×4 blocks. One configuration consists of the product of one single-particle electron and one single-particle-hole state leading to a 4×4 matrix when spin is included. This corresponds roughly to the Hartree-Fock level,[43] which exactly neglects correlations. The results for the absorption at this level are given in Fig. 10(b). In the last step we include coupling between the configurations via configuration interaction where all the available confined levels are utilized. The results are given in Fig. 10(c). While this last step represents the limit of the present approach and is sometimes referred to as "full CI," it likely misses some of the correlations.

In Fig. 10 we notice that the entire spectrum is shifted to the red when Coulomb interactions are introduced [difference between Figs. 10(a) and 10(b)]. This is expected since the electron-hole attraction in these structures extends between 0 and 7 meV, depending on the considered states. As we can expect from the extent of the wave functions (Fig. 7) the transitions between the states e_i and h_j, where the indices i and j are equal, are bright. These are labeled as $s1$–$s4$ for e_0h_0, e_1h_1, e_2h_2, and e_3h_3, respectively. However, several other transitions lead to significant oscillator strength, as for instance e_0h_1, labeled as $s5$ in Fig. 10(b). The inclusion of correlations leads to a dramatic modification of the spectrum [difference between Fig. 10(b) and 10(c)] where we recover the results from Figs. 8(c) and 8(f) with the four strongest peaks $a1$–$a4$. Most of the bright transitions at the single-configuration level become dark and the states rearrange

themselves to lead to a simple spectrum, where the lowest energy transitions is shifted by a correlation energy of more than 3 meV. The analysis of the origin of the lowest energy peak $a1$ shows that it is to 60% given by the e_0h_0 configuration with an admixture of 40% from several other configu-

TABLE V. Compiled reference bulk properties and empirical pseudopotential results for AlAs using the parameters from Table IV.

	LB[a]	Review[b]	LCAO[c,d]	GW[e]	Used target	EP results
$\varepsilon(\Gamma_{1v})$			−11.95/−11.87	−12.41	−12.41	−12.53
$\varepsilon(\Gamma_{15v})$	0.0	0.0	0.0	0.0	−6.00	−6.00
$\varepsilon(\Gamma_{1c})$	3.10	3.099	2.79/2.81	2.88	3.10	3.09
$\varepsilon(\Gamma_{15c})$			4.48/4.21	5.14	5.14	4.49
$\varepsilon(X_{1v})$			−9.63/−9.80	−10.41	−10.41	−8.77
$\varepsilon(X_{3v})$	−5.7		−5.69/−5.52	−5.87	−5.70	−7.83
$\varepsilon(X_{5v})$	−2.32		−2.38/−2.32	−2.44	−2.32	−2.34
$\varepsilon(X_{1c})$	2.23	2.24	2.37/2.21	2.14	2.25	2.24
$\varepsilon(X_{3c})$	2.43		3.84/2.89	3.03	2.43	3.02
$\varepsilon(L_{1v})$			−10.28/−10.43	−10.97	−10.97	−10.27
$\varepsilon(L_{2v})$			−5.95/−6.41	−6.01	−6.01	−6.76
$\varepsilon(L_{3v})$			−0.88/−0.97	−3.90	−0.88	−0.95
$\varepsilon(L_{1c})$	2.57	2.46	2.81/2.48	2.91	2.46	2.57
$\varepsilon(L_{3c})$			5.86/4.87	5.59	5.59	5.59
$m_e^*(\Gamma_{1c})$	0.15	0.15			0.15	0.149
$m_e^*(L_{1c,l})$	1.32	1.32				
$m_e^*(L_{1c,t})$	0.15	0.15				
$m_e^*(X_{1c,l})$	1.1	0.97				
$m_e^*(X_{1c,t})$						

rize experimental results for TFQDs in GaAs wells of different thicknesses. The values obtained experimentally for the negative trion shift for different well width are similar and lie around 3 meV, besides for very thick 50 ML wells where it drops to 1.2 meV. One possible reason for our underestimated trion shifts is the limited amount of correlations we can include in the CI basis due to the limited number of confined levels. This hypothesis is reinforced by the fact that path-integral Monte Carlo calculations[22,45] where correlations are fully taken into account (while the single-particle Hamiltonian is solved at the effective-mass level) do yield binding energies between 1.5 and 4.0 meV depending on the radius of the monolayer fluctuation (a cylindrical dot was assumed). Our results for the fine-structure splittings is too low compared to the experimental evidence, as already discussed.

XIII. CONCLUSIONS

We used the atomistic empirical pseudopotential method and configuration interaction to calculate the electronic and optical properties of thickness-fluctuation quantum dots (sometimes called *natural* quantum dots). These structures confined the electron and hole wave function through a single atomic monolayer step in a quantum well. These atomistic calculations require the treatment of up to five million atoms for the largest structure of 100 by 20 nm. We first present results for $GaAs/Al_{0.3}Ga_{0.7}As$ quantum wells where

[1] A. Zrenner, L. V. Butov, M. Hagn, G. Abstreiter, G. Böhm, and G. Weimann, Phys. Rev. Lett. **72**, 3382 (1994).
[2] K. Brunner, G. Abstreiter, G. Böhm, G. Tränkle, and G. Weimann, Phys. Rev. Lett. **73**, 1138 (1994).
[3] K. Brunner, G. Abstreiter, G. Böhm, G. Tränkle, and G. Weimann, Appl. Phys. Lett. **64**, 3320 (1994).
[4] H. F. Hess, E. Betzig, T. D. Harris, L. N. Pfeiffer, and K. W. West, Science **264**, 1740 (1994).
[5] J. Hours, P. Senellart, E. Peter, A. Cavanna, and J. Bloch, Phys. Rev. B **71**, 161306(R) (2005).
[6] P. Senellart, E. Peter, J. Hours, A. Cavanna, and J. Bloch, Phys. Rev. B **72**, 115302 (2005).
[7] D. Gammon, E. S. Snow, B. V. Shanabrook, D. S. Katzer, and D. Park, Phys. Rev. Lett. **76**, 3005 (1996).
[8] E. Ivchenko, Phys. Status Solidi A **164**, 487 (1997).
[9] S. Gupalov, E. Ivchenko, and A. Kavokin, J. Exp. Theor. Phys. **86**, 388 (1998).
[10] Q. Wu, R. D. Grober, D. Gammon, and D. S. Katzer, Phys. Rev. B **62**, 13022 (2000).
[11] J. Guest, T. Stievater, G. Chen, E. Tabak, B. Orr, D. Steel, D. Gammon, and D. Katzer, Science **293**, 2224 (2001).
[12] D. Gammon, A. L. Efros, T. A. Kennedy, M. Rosen, D. S. Katzer, D. Park, S. W. Brown, V. L. Korenev, and I. A. Merkulov, Phys. Rev. Lett. **86**, 5176 (2001).
[13] J. G. Tischler, A. S. Bracker, D. Gammon, and D. Park, Phys. Rev. B **66**, 081310(R) (2002).
[14] G. Chen, T. H. Stievater, E. T. Batteh, X. Li, D. G. Steel, D. Gammon, D. S. Katzer, D. Park, and L. J. Sham, Phys. Rev. Lett. **88**, 117901 (2002).
[15] J. Hours, S. Varoutsis, M. Gallart, J. Bloch, I. Robert-Philip, A. Cavanna, I. Abram, F. Laruelle, and J. M. Gerard, Appl. Phys. Lett. **82**, 2206 (2003).
[16] K. Matsuda, T. Saiki, S. Nomura, M. Mihara, Y. Aoyagi, S. Nair, and T. Takagahara, Phys. Rev. Lett. **91**, 177401 (2003).
[17] A. S. Bracker *et al.*, Phys. Rev. Lett. **94**, 047402 (2005).
[18] T. Unold, K. Mueller, C. Lienau, T. Elsaesser, and A. D. Wieck, Phys. Rev. Lett. **94**, 137404 (2005).
[19] J. Berezovsky, O. Gywat, F. Meier, D. Battaglia, X. Peng, and D. D. Awschalom, Nat. Phys. **2**, 831 (2006).
[20] C. Riva, F. M. Peeters, and K. Varga, Phys. Rev. B **61**, 13873 (2000).
[21] L. C. O. Dacal and J. A. Brum, Phys. Rev. B **65**, 115324 (2002).
[22] A. V. Filinov, C. Riva, F. M. Peeters, Y. E. Lozovik, and M. Bonitz, Phys. Rev. B **70**, 035323 (2004).
[23] S.-S. Li, K. Chang, and J.-B. Xia, Phys. Rev. B **71**, 155301 (2005).
[24] P. N. Keating, Phys. Rev. **145**, 637 (1966).
[25] A. J. Williamson, L.-W. Wang, and A. Zunger, Phys. Rev. B **62**, 12963 (2000).
[26] A. J. Williamson and A. Zunger, Phys. Rev. B **59**, 15819 (1999).
[27] L.-W. Wang and A. Zunger, Phys. Rev. B **59**, 15806 (1999).
[28] A. Szabo and N. S. Ostlund, *Modern Quantum Chemistry* (McGraw-Hill, New York, 1989).
[29] A. Franceschetti, H. Fu, L.-W. Wang, and A. Zunger, Phys. Rev. B **60**, 1819 (1999).
[30] R. Resta, Phys. Rev. B **16**, 2717 (1977).
[31] S. Guha, A. Madhukar, and K. C. Rajkumar, Appl. Phys. Lett. **57**, 2110 (1990).
[32] D. Bimberg, M. Grundmann, and N. N. Ledentsov, *Quantum Dot Heterostructures* (Wiley, New York, 1999).
[33] D. Bimberg, F. Heinrichsdorff, R. K. Bauer, D. Gerthsen, D. Stenkamp, D. E. Mars, and J. N. Miller, J. Vac. Sci. Technol. B **10**, 1793 (1992).
[34] R. F. Kopf, E. F. Schubert, T. D. Harris, R. S. Becker, and G. H. Gilmer, J. Appl. Phys. **74**, 6139 (1993).
[35] V. Savona and W. Langbein, Phys. Rev. B **74**, 075311 (2006).
[36] M. Erdmann, C. Ropers, M. Wenderoth, R. G. Ulbrich, S. Malzer, and G. H. Dohler, Phys. Rev. B **74**, 125412 (2006).
[37] A. Rudra, E. Pelucchi, D. Oberli, N. Moret, B. Dwir, and E. Kapon, J. Cryst. Growth **272**, 615 (2004).
[38] B. Courboules, C. Deparis, J. Massies, M. Leroux, and C. Grattepain, Appl. Phys. Lett. **65**, 836 (1994).
[39] G. Bastard, *Wave Mechanics Applied to Semiconductor Heterostructures* (Halstead, New York, 1988).
[40] A. G. Norman, M. C. Hanna, P. Dippo, D. H. Levi, R. C. Reedy, J. S. Ward, and M. M. Al-Jassim, in *Proceedings of 31st IEEE Photovoltaic Specialists Conference, Lake Buena Vista, Florida, USA* (IEEE, New York, 2005), pp. 43–48.
[41] P. Yu and M. Cardona, *Fundamentals of Semiconductors* (Springer, Berlin, 2001).
[42] G. Bester, S. Nair, and A. Zunger, Phys. Rev. B **67**, 161306(R) (2003).
[43] L. X. He, G. Bester, and A. Zunger, Phys. Rev. B **72**, 195307 (2005).
[44] S. Kalliakos, M. Rontani, V. Pellegrini, C. Garcia, A. Pinczuk, G. Goldoni, E. Molinari, L. Pfeiffer, and K. West, Nat. Phys. **4**, 467 (2008).
[45] A. S. Bracker *et al.*, Phys. Rev. B **72**, 035332 (2005).
[46] G. Weisz, Phys. Rev. **149**, 504 (1966).
[47] M. S. Hybertsen and S. G. Louie, Phys. Rev. B **34**, 2920 (1986).
[48] *Numerical Data and Functional Relationships in Science and Technology*, Landolt-Börnstein, New Series, Group III, Vols. 17, 22, and 41, Pt. A, edited by U. Madelung, M. Schultz, and H. Weiss (Springer-Verlag, Berlin, 1997).
[49] I. Vurgaftman, J. R. Meyer, and L. R. Ram-Mohan, J. Appl. Phys. **89**, 5815 (2001).
[50] M. Huang and W. Y. Ching, J. Phys. Chem. Solids **46**, 977 (1985).
[51] A. Chen and A. Sher, Phys. Rev. B **22**, 3886 (1980).
[52] X. Zhu and S. G. Louie, Phys. Rev. B **43**, 14142 (1991).
[53] S. H. Wei and A. Zunger, Phys. Rev. B **60**, 5404 (1999).